NASA TECHNICAL NOTE

NASA TN D-7006

DESIGN STUDY OF SHAFT FACE SEAL WITH SELF-ACTING LIFT AUGMENTATION

II - Sealing Dam

by John Zuk, Lawrence P. Ludwig, and Robert L. Johnson

Lewis Research Center
Cleveland, Ohio 44135

NATIONAL AERONAUTICS AND SPACE ADMINISTRATION • WASHINGTON, D. C. • NOVEMBER 1970

1. Report No.	2. Government Accession No.	3. Recipient's Catalog No.
NASA TN D-7006		

4. Title and Subtitle	5. Report Date
DESIGN STUDY OF SHAFT FACE SEAL WITH SELF-ACTING LIFT AUGMENTATION II - SEALING DAM	November 1970
	6. Performing Organization Code
7. Author(s)	8. Performing Organization Report No.
John Zuk, Lawrence P. Ludwig, and Robert L. Johnson	E-5796
	10. Work Unit No. 126-15
9. Performing Organization Name and Address	11. Contract or Grant No.
Lewis Research Center National Aeronautics and Space Administration Cleveland, Ohio 44135	
	13. Type of Report and Period Covered
12. Sponsoring Agency Name and Address	Technical Note
National Aeronautics and Space Administration Washington, D. C. 20546	14. Sponsoring Agency Code

15. Supplementary Notes

16. Abstract

Analytical studies made on a 6.50-inch (16.5-cm) nominal dam diameter seal with sealed pressure to 315 psia (217 N/cm^2 abs) revealed that a shaft face seal with self-acting lift pads can be designed to yield low leakage and positive sealing face separation. The study showed that the leakage flow through the sealing faces can become choked at pressure ratios as low as 4 to 1 for typical seal operating film thicknesses. Slight angular deformations of the sealing faces had a significant effect on the pressure gradient within the sealing faces; thus, seal force balance was correspondingly affected. For sealing faces having angular deformation, the radial width of the sealing dam was found to markedly affect the seal force balance.

17. Key Words (Suggested by Author(s))		18. Distribution Statement
Sealing dam	Gas film seal	Unclassified - unlimited
Face seal	Self-acting geometry	
Gas bearings	Seal	

19. Security Classif. (of this report)	20. Security Classif. (of this page)	21. No. of Pages	22. Price*
Unclassified	Unclassified	28	$3.00

*For sale by the Clearinghouse for Federal Scientific and Technical Information
Springfield, Virginia 22151

DESIGN STUDY OF SHAFT FACE SEAL WITH SELF-ACTING LIFT AUGMENTATION

II - SEALING DAM

by John Zuk, Lawrence P. Ludwig, and Robert L. Johnson

Lewis Research Center

SUMMARY

A design study was made of the sealing dam portion of a shaft face seal with self-acting lift augmentation. This type of seal has potential use in advanced aircraft gas turbines. A 6.50-inch (16.5-cm) nominal diameter dam, typical of sump seals in aircraft gas turbines, with sealed pressures of 65, 215, and 315 psia (45, 148, and 217 N/cm^2 abs) was considered. In this parametric study, the leakage flow rate, pressure gradient, opening force, and center of pressure as well as the effects of sealing face deformation were investigated.

The study showed that this seal can be designed to yield low leakage and yet maintain positive sealing face separation; hence, an order of magnitude less leakage and more compact design is possible as compared to conventional labyrinth seal - face seal practice.

In addition, the study also showed that the gas leakage flow can become choked at pressure ratios as low as 4 to 1 for typical sealing gaps at operating conditions. Slight face angular deformation (i.e., ±0.001 rad) had a significant effect on the pressure gradient within the sealing faces; thus, the seal force balance (opening force and center of pressure) was markedly affected. The seal opening force is also significantly affected by the width of the sealing dam when slight angular face deformation is present.

INTRODUCTION

Shaft seal systems in advanced aircraft turbine engines will be operated at speeds, temperatures, and pressures higher than those currently used.

Conventional face seals presently in use in some gas turbine engines are limited to a sliding velocity of about 350 feet per second (107 m/sec), a gas temperature of 800° F (700 K), and a pressure of 125 psi (86.1 N/cm^2) (ref. 1). Advanced engines, however,

require seals to operate at 500 feet per second (152 m/sec) (ref. 2), and at pressures to 500 psi (344 N/cm^2) and temperatures to 1300° F (977 K) (ref. 3). For face seals to operate at these conditions, a positive face separation (no rubbing contact) will be required in order to achieve long life and reliability.

Some conventional face seals used in current engines most likely operate with positive face separation under steady-state conditions, but this positive face separation is not assured by the design procedure. Extension of the speed, pressure, and temperature ranges of the conventional face seal, therefore, will be minimal unless the design ensures the small but vital positive sealing face separation necessary for long life and reliability. Labyrinth seals could also be used in some applications; however, the operating clearance is inherently large due to thermal, centrifugal, and mechanical radial growth and radial vibrations. Another approach where a conventional face seal may still be used in some applications is the face seal - labyrinth seal system shown in figure 1.

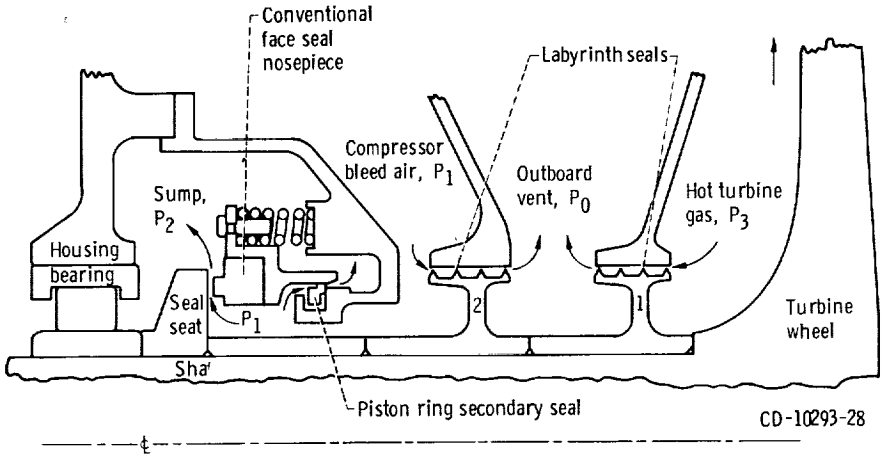

Figure 1. - Schematic of typical gas turbine seal systems (not to scale).

The proposed approach, however, is the use of gas film seals with self-acting lift augmentation (see fig. 2 and the section BACKGROUND). In this report we will look critically at the sealing dam.

The design of a gas film seal requires a compromise on the operating film thickness. The film thickness must be small enough so that the leakage is a minimum but it must be large enough so that power dissipation, accompanying shear heating, and face deformation is tolerable. Also the film thickness must be large enough so that the gas film is operating in the continum flow regime where its film stiffness is the highest. The geometric design is also a compromise due to variable operating conditions encountered in flight, such as takeoff and climb, cruise, and descent.

The objective of this study was to determine if the shaft face seal with self-acting lift augmentation was feasible and able to replace the conventional labyrinth and face seal systems in advanced aircraft gas turbines. To achieve this objective the following factors were determined: (1) leakage rates, (2) the effect of sealing face deformation on seal opening force, and (3) the effect of sealing face radial width (dam) changes on opening force and leakage.

The parametric study was made on a face seal with self-acting lift pads having a 6.5-inch (16.5-cm) nominal dam diameter. Sealed gas pressures at three representative design points of advanced aircraft gas turbine operation were considered. Leakage rates for various sealing gap heights were calculated, and the effects of sealing face deformation and seal face radial width dam were evaluated.

BACKGROUND

Figure 1 depicts schematically (not to scale) a mainshaft seal system at the turbine location. This seal system consists of a conventional rubbing-contact face seal and conventional labyrinth seals. The face seal consists of the rotating seat (attached to the shaft) and a nonrotating carbon-graphite nose (and its retainer) which can move in an axial direction to accommodate engine thermal growth. Compressor bleed air (P_1) from early stages (or from the fan) establishes a higher pressure at the inside diameter of the carbon-graphite nose than in the bearing sump; gas leakage through the seal into the sump helps prevent oil leakage out. The compressor bleed air from the early stages also leaks through a labyrinth seal (fig. 1) into an overboard vent (P_0) which thermally protects the sump from the hot, high-pressure gas (P_3) (in the turbine region). This hot, high-pressure gas leaks through a labyrinth seal into the overboard vent and this leakage represents an efficiency penalty in high-pressure engines. Replacement of this labyrinth seal and the conventional sump face seal system with face seals having positive sealing face separation would improve overall engine efficiency by decreasing leakage and increasing seal system operating pressure and speed capability.

A direct approach to obtaining positive sealing face separation is found in the hydrostatic and self-acting seal designs under investigation in the studies reported in references 4 and 5. The self-acting seal design, which has a low leakage potential (ref. 5), is a conventional face seal with self-acting pad geometry (step-type gas-lubricated bearings) for lift augmentation (see fig. 2). It should be noted that, in the conventional face seal, divergent sealing faces lead to loss of seal opening force; hence, rubbing contact can occur (ref. 5). However, as pointed out in reference 5, the step-type gas bearing added to a conventional face seal acts to maintain sealing surface separation even though divergent sealing face deformation occurs. The feasibility of the self-acting face seal

has been demonstrated in several NASA-sponsored programs (ref. 5). Recent data show satisfactory performance to a speed of 450 feet per second (122 m/sec), a pressure of 250 psi (172 N/cm^2), and a sealed gas temperature of 1200° F (810 K).

The design of the self-acting geometry is vital to seal dynamic performance. The self-acting geometry must provide

(1) Sufficient lift force to separate the surfaces at less than idle speed

(2) Sufficient gas film stiffness to make the nosepiece dynamically track the axial motions of the seal seat face

A necessary step in optimization of lift augmentation in a face seal is a parametric study of the self-acting geometry. This was done in a companion paper, reference 6. The load-carrying capacity of the self-acting geometry was calculated for various pad recess depths, film thicknesses, and angular deformations, and for a number of self-acting pads. The self-acting geometry resulting from this study is shown in figure 2(b).

The sealing dam (fig. 2) is that portion of the self-acting gas film shaft seal where the pressure drop and gas leakage occur. Since the seal is pressure-balanced, precise knowledge of the pressure drop across the sealing dam and of the lift pad force is essential in determining the seal force.

Description of Face Seal With Self-Acting Geometry

Figure 2 shows a face-type seal with a self-acting pad geometry that consists of a series of shallow recesses arranged circumferentially around the seal inside the sealing dam. It should be noted that the lift geometries are bounded at the inside and outside diameters by the sealed pressure P_1. This is accomplished by feed slots that connect the annular groove directly inside the sealing dam with the sealed pressure in the cavity. Since each lift pad is completely surrounded by the sealed pressure, no pressure drop occurs in the pad region because of seal leakage. Pressure drop due to seal leakage occurs only across the sealing faces (dam) on the primary sealing face (and across the piston ring secondary seal (see fig. 1) but this is not germane to this study). The secondary seal (fig. 1) friction was not considered since the primary objectives were to investigate the effects of sealing face deformation and dam width on seal leakage and operating film thickness.

The effect of the self-acting geometry on face seal operation is illustrated in figure 2(a), which shows parallel sealing faces operating without rubbing contact because of a balance between the closing force and the opening force, that is, the self-acting lift force plus the pressure acting between the sealing faces. If the seal tends to close, the gas bearing force increases to prevent rubbing contact; thus, a condition of no rubbing contact can prevail except at startup and shutdown.

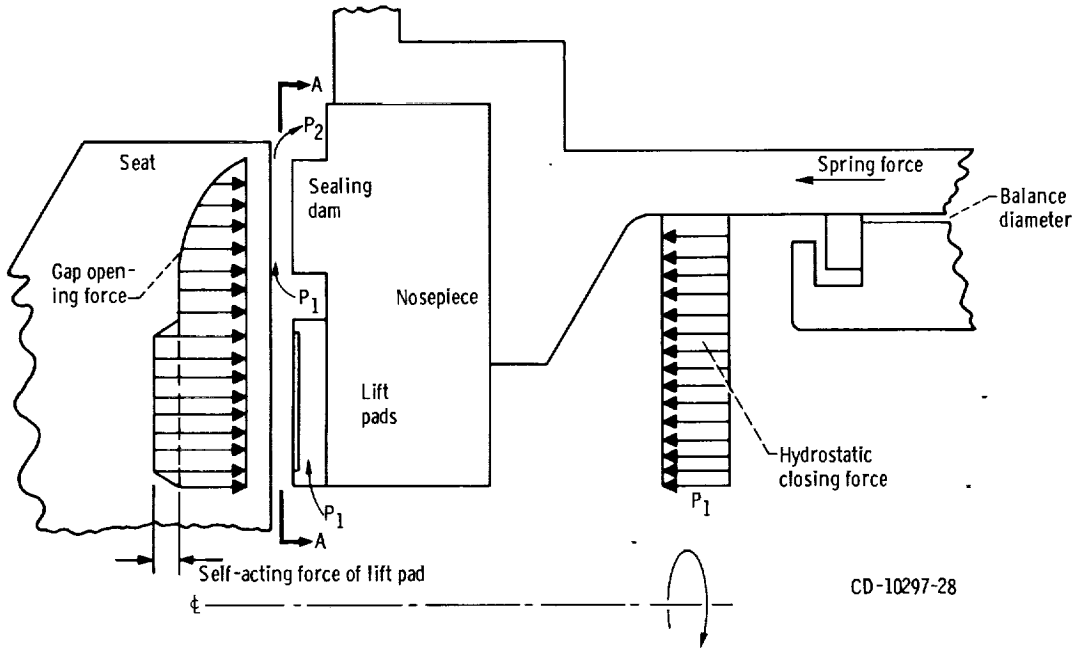

(a) Mechanical, pneumatic, and self-acting forces on seal nosepiece.

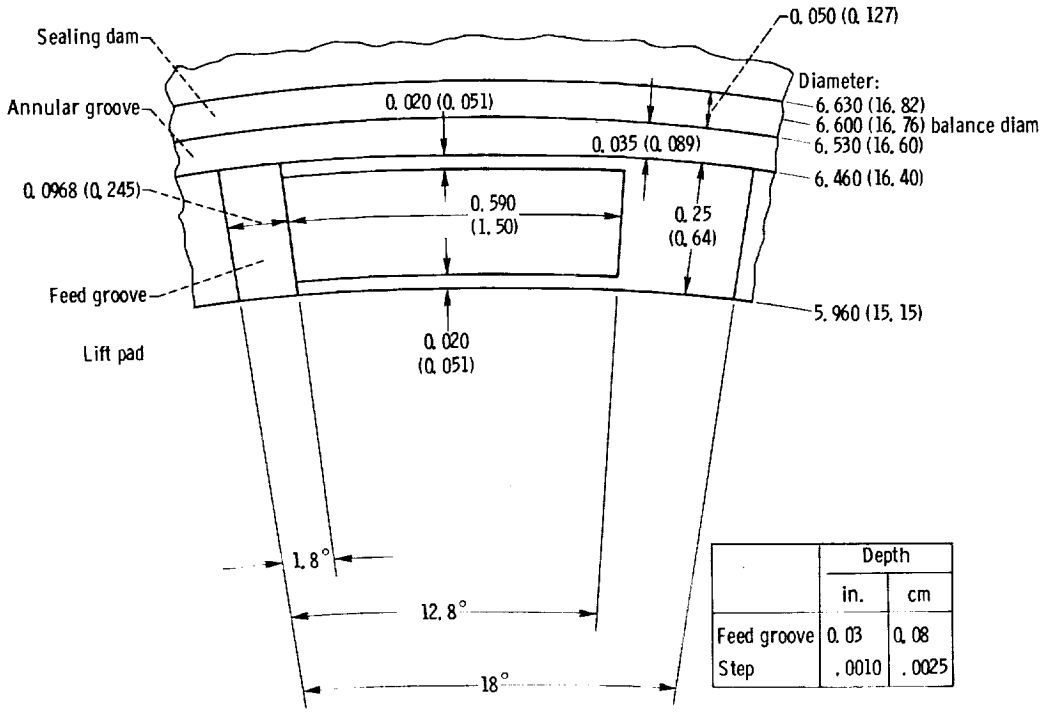

	Depth	
	in.	cm
Feed groove	0.03	0.08
Step	.0010	.0025

(b) Section A-A: Details of sealing dam and self-acting pad geometry. All dimensions are in inches (cm).

Figure 2. - Face seal with self-acting lift pads.

TABLE I. - DESIGN POINTS - REPRESENTATIVE OF ADVANCED AIRCRAFT GAS TURBINE OPERATION

	Design points		
	1	2	3
Operating condition simulated	Descent	Takeoff and climb	Cruise
Velocity (mean relative surface speed of seal dam surfaces), V, ft/sec (m/sec)	200 (61)	500 (153)	450 (137)
Sealed gas pressure, P_1, psia (N/cm^2 abs)	65 (45)	215 (148)	315 (217)
Sealed gas temperature, T_1, ^{o}F (K)	100 (311)	800 (700)	1300 (977)
Sump pressure, P_2, psia (N/cm^2 abs)	15 (10.3)	15 (10.3)	15 (10.3)
Viscosity of air, ρ, lbf-sec/in.^{2} (N-sec/cm^2)	2.75×10^{-9} (1.9×10^{-10})	4.87×10^{-9} (3.36×10^{-10})	6.00×10^{-9} (4.14×10^{-10})

Design Points

For the purpose of analysis, three design points were selected as representative of operating conditions in the advanced gas turbine (see table I). These design points simulate engine conditions at takeoff and climb, cruise, and descent. The sump pressure was chosen to be 15 psia (10.3 N/cm^2 abs) since this pressure could be readily maintained in laboratory experiments. In an actual engine, the sump pressure would be about the same as the ambient pressure, which depends on altitude and atmospheric conditions. The seal is internally pressurized. In sump seals, the oil-gas mixture is located at the sealing dam outside diameter to preclude oil leakage caused by centrifugal force.

Sealing Dam Design Analysis

The sealing dam analysis is based on a sealing dam model described in reference 7. The model consists of two parallel, coaxial, circular rings in relative rotation at a constant speed separated by a very narrow gap (fig. 3). A pressure differential exists between the ring's inner and outer radii. The cavities on either side (i.d. and o.d.) of the sealing dam are assumed to be constant-pressure reservoirs.

Refer to reference 7 for details of the assumptions; however, the following pertinent comments should be noted:

(1) The effect of the rotational flow on the hydrostatic radial flow is neglected. This

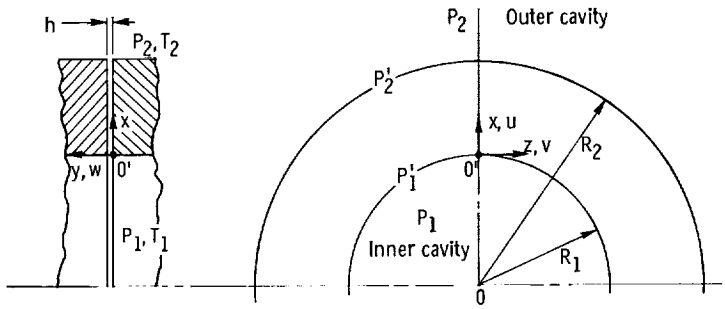

(a) Parallel sealing faces.

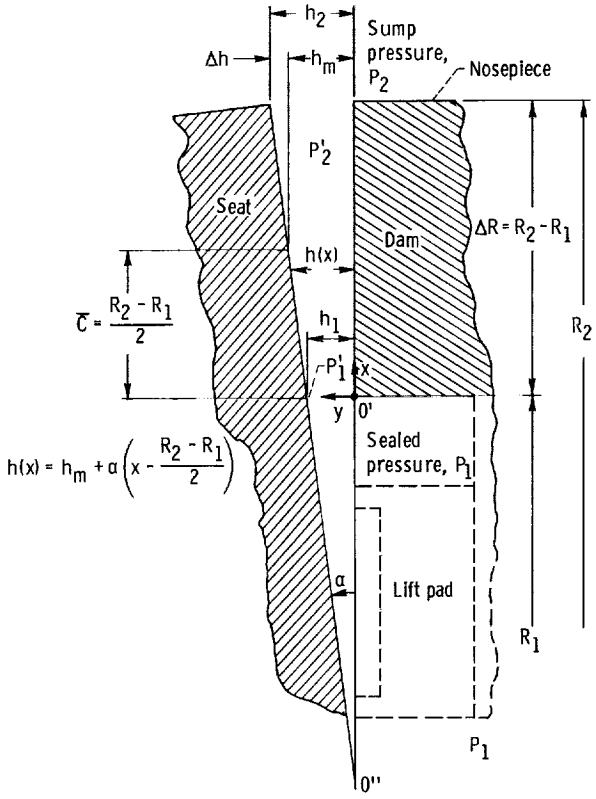

(b) Sealing faces with small tilt (face deformation).

Figure 3. - Model and notation of sealing faces (dam).

TABLE II. - SUMMARY OF SUBSONIC FLOW EQUATIONS FROM REFERENCE 7

Leakage flow rate	$Q = \begin{Bmatrix} 2.726 \\ 0.001287 \end{Bmatrix} \frac{h_{char}^3 L\left(P_1^2 - P_2^2\right)}{\mu \mathcal{R} T (R_2 - R_1)}, \begin{Bmatrix} SCFM \\ SCMS \end{Bmatrix}$
Pressure distribution:	
Parallel film case	$P = P_2 \left[1 - \left(1 - \frac{P_1^2}{P_2^2} \right) \left(\frac{R_2 - r}{R_2 - R_1} \right) \right]^{1/2}$
Small deformation case	$P = P_1 \left\{ 1 + \frac{\left[\left(\frac{P_2}{P_1} \right)^2 - 1 \right] h_2^2 x (2B + \alpha x)}{(R_2 - R_1) h_m (B + \alpha x)^2} \right\}^{1/2}$
Sealing dam force:	
Parallel film case	$F = \frac{2 P_1 L (R_2 - R_1) \left[1 - \left(\frac{P_2}{P_1} \right)^3 \right]}{3 \left[1 - \left(\frac{P_2}{P_1} \right)^2 \right]}$
Small deformation case	$F = L \int_0^{R_2 - R_1} (P - P_{min}) dx$ (evaluated numerically)
Radial center of pressure:	
Parallel film case	$R_c = \frac{L (R_2 - R_1)^2}{F} \left\{ \frac{P_1 \left[\frac{2}{5} \left(\frac{P_2}{P_1} \right)^5 - \frac{2}{3} \left(\frac{P_2}{P_1} \right)^3 + \frac{4}{15} \right]}{\left[1 - \left(\frac{P_2}{P_1} \right)^2 \right]^2} - \frac{P_{min}}{2} \right\}$
Small deformation case	$R_c = \frac{L}{F} \int_0^{R_2 - R_1} (P - P_{min}) x \, dx$ (evaluated numerically)

assumption is justified by using equation (39) from reference 8. For the range of film thickness considered, the increase in leakage due to rotation would only be 2.6, 7.9, and 4.3 percent for design points 1, 2, and 3, respectively.

(2) For subsonic flow, Mach number $\leq 1/\sqrt{\gamma}$, the analysis of reference 7 is used. This analysis finds an exact solution for this case when the viscous friction is balanced by the pressure drop. For this condition the entrance pressure drop is small; hence, $P_1 = P_1'$ and $P_2 = P_2'$ (see fig. 3). The flow is basically isothermal for the film thickness range studied. Neglecting rotation, it can be shown theoretically that the isothermal and adiabatic flow solutions are identical. This analysis yields the classical cubic dependence of mass flow on film thickness. Also this analysis enables small tilts of the sealing dam surfaces to be studied. These small tilts simulate seal face deformation which can occur as a result of, for example, thermal and centrifugal effects. The equations used for this analysis are summarized in table II.

(3) For flow approaching Mach 1, where the flow chokes, the inertia force neglected in reference 7 becomes important. Also the flow behaves more as an adiabatic flow than as an isothermal flow. The mathematics is very complex because of the nonlinearity of the inertia terms; thus, an approximate analytical model must be used. In this model the flow is analyzed as a quasi-one-dimensional flow utilizing a control volume integral analysis. The viscous effect is represented by a mean friction factor which has been observed to be almost invariant under many an ensemble of fluid mechanics experiments, geometries, and conditions. (Details of this analysis are available from the authors.) For the purposes of this analysis, a mean friction factor of $\bar{f} = 24/Re$ will be used. This friction factor can be derived from the exact analysis of reference 7 for subsonic flow.

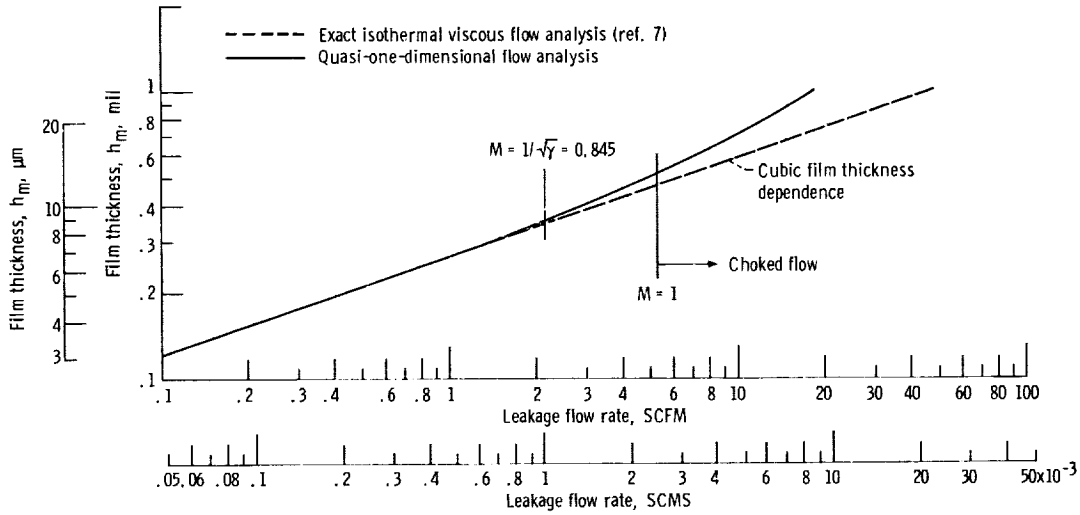

Figure 4. - Seal gas leakage as function of film thickness for parallel sealing dam surfaces. Design point 1: Radial dam width, ΔR, 50 mils (0.127 cm); sealed air pressure, P_1, 65 psia (45 N/cm^2 abs); sump pressure, P_2, 15 psia (10.3 N/cm^2 abs); seated gas temperature, T_1, 100° F (311 K).

Figure 4 shows that the leakage flow rate analysis of reference 7 and the quasi-one-dimensional analysis coincide until the Mach number exceeds 0.845, at which point the isothermal viscous flow model loses its validity. This model is valid for choked flow. The flow is choked at the exit. The area expansion is negligible in this design (i.d./o.d. = 0.985). For purposes of this design study, the effects of different surface temperatures and of the heat source in the fluid film due to rotation are neglected. In this case, it will be shown that there is a pressure drop at the entrance ($P_1' \neq P_1$) and that, due to choking at the exit, $P_2' \neq P_2$.

RESULTS

The results that are found were obtained by using the computer program found in reference 7 and a computer program carrying out the quasi-one-dimensional analysis available from the authors. These analyses appeared to be the best available models simulating the actual gas film seal.

The design of the gas film seal required finding a film thickness small enough so the leakage is a minimum but yet large enough that both the power dissipation and subsequent shear heating are tolerable and potential seal face deformations can be accommodated. A rough calculation showed the gap must be at least 0.1 mil (0.00025 cm) for parallel surfaces. A larger gap than 0.1 mil (0.00025 cm) is necessary to accommodate deformation of the sealing faces. Initial screening of the sealing dam radial width ΔR on force balance suggested that radial widths of 20, 50, 80, and 100 mils (0.051, 0.127, 0.203, and 0.254 cm) be investigated in detail. Leakage flow rates not exceeding 25 standard cubic feet per minute (SCFM) (1.18×10^{-3} std m^3/sec (SCMS)) were desired for all three design points.

Leakage Flow Rates

Figure 4 shows the relation between film thickness and gas leakage flow from the high-pressure side into the sump (low-pressure side). The calculations for 65 psia (45 N/cm^2 abs) and 100° F (311 K) (design point 1, table I) were obtained from the seal analysis computer programs and are for parallel surfaces and a sealing dam of 50 mils (0.127 cm) in radial width. For small film thickness (0.2 mil, 0.0005 cm) the leakage is small, in the range of 0.43 SCFM (2.06×10^{-4} SCMS). But because of the cubic dependence of leakage on film thickness, a slight change in film thickness significantly affects leakage. Even though the pressure ratio is approximately 4 to 1, choking occurs for a film thickness of 0.52 mil (0.00131 cm). For gaps larger than 0.3 mil (0.000756 cm) the leakage has a lesser than cubic dependence on gap. The limiting case would be a linear dependence which would be achieved when the film thickness is of the order of

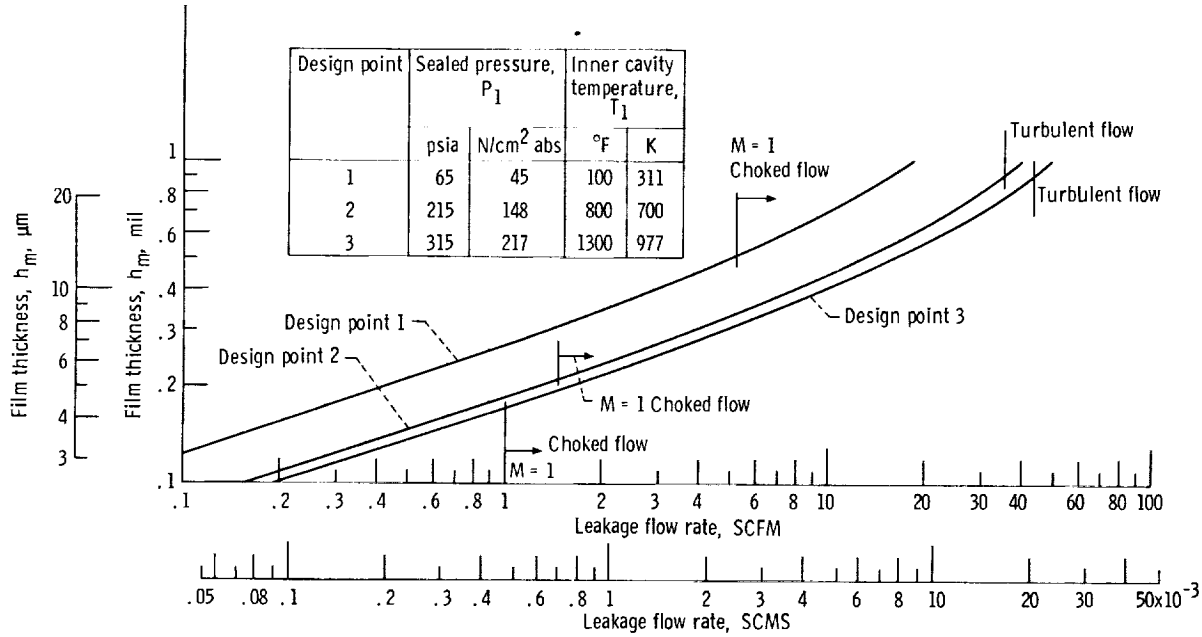

Figure 5. - Effect of operating point (pressure and temperature) on seal gas leakage. Parallel sealing surfaces; sealing face radial length, 50 mils (0.127 cm); sump pressure, P_2, 15 psia (10.3 N/cm^2 abs); sealed fluid, air.

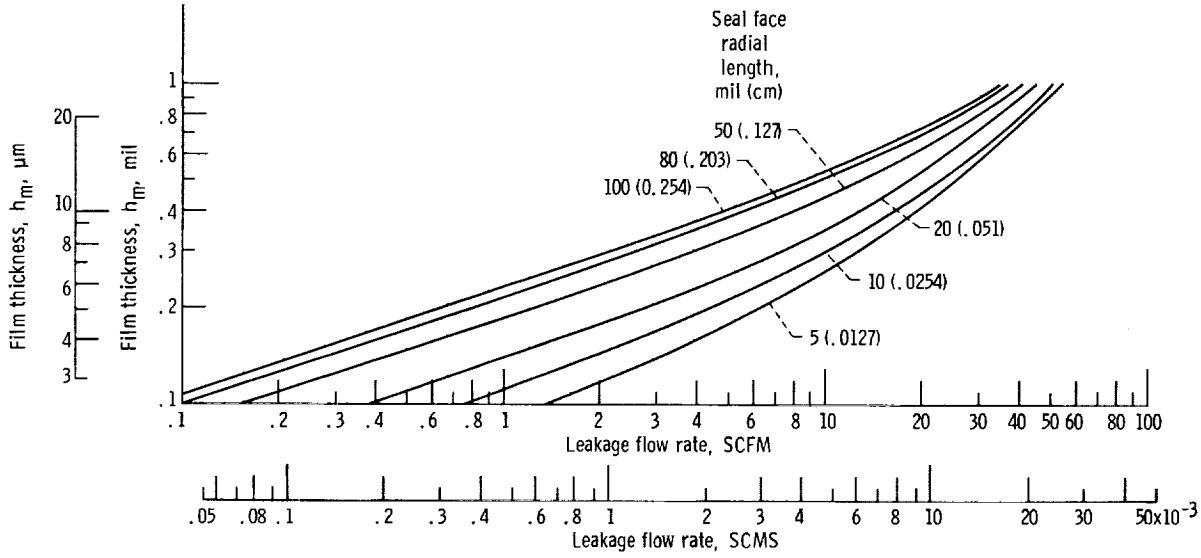

Figure 6. - Effect of seal face radial length on seal leakage. Parallel sealing faces; design point 2: sump pressure, P_2, 15 psia (10.3 N/cm^2 abs); sealed pressure, P_1, 215 psia (148 N/cm^2 abs); sealed gas temperature, 800° F (700 K); sealed fluid, air.

the sealing dam radial width of 50 mils (0.127 cm). This would be a choked orifice flow which linearly varies with film thickness.

Figure 5 shows the effects of operating pressure and temperature on seal leakage for parallel sealing surfaces for the three design points. Choking occurs at film thicknesses of 0.52, 0.22, and 0.17 mil (0.00131, 0.00054, and 0.000429 cm) for design points 1, 2, and 3, respectively. Also transition to turbulence has occurred for design points 2 and 3 at a film thickness of 0.9 mil (0.00227 cm). The radial flow Reynolds number has exceeded 2300. This Reynolds number, based on hydraulic diameter, has been chosen to be the critical transition Reynolds number.

Figure 6 shows the effect of sealing dam radial width on leakage flow at design point 2. The four radial widths of 20, 50, 80, and 100 mils (0.051, 0.127, 0.203, and 0.254 cm) are those used in this study. Also shown are 5-mil (0.0127-cm) and 10-mil (0.0254-cm) radial width dams. These plots illustrate that, from strictly a leakage point of view, the longest leakage path possible is most desirable. However, it will be shown that the leakage path length must be compromised from a force balance point of view when surface deformations occur.

Pressure Gradients

Figure 7 shows, for parallel sealing faces, the normalized pressure as a function of radial position within the sealing gap: The normalized pressure gradients for the three operating design points (see table I) are shown; since the faces are parallel, the profile is independent of film thickness. However, the profiles shown are valid only below the choking points (Mach number <0.845).

For nonparallel sealing surfaces, the pressure gradients are dependent on film thickness. This is shown in figure 8 for the design point of 65 psia (45 N/cm^2 abs) and 100° F (311 K). The pressure gradients are plotted for mean film thicknesses of 0.2 mil (0.00051 cm) and 0.4 mil (0.00102 cm) and for a sealing face deformation of ± 0.001 radian. (The negative (-) deformation indicates a converging film in the leakage direction, and a positive (+) deformation indicates a diverging film.) The important point (see fig. 8) is that for the convergent film case, a decrease in film thickness results in greater area (larger opening force) under the pressure gradient curve; thus, the convergent film has a positive film stiffness. Conversely, as shown by figure 8, a divergent film has a negative film stiffness. This means that for a divergent film a decrease in film thickness (which always occurs dynamically) will cause a decrease in opening force. This decrease must be counterbalanced by a corresponding increase in lift force of the self-acting pads if a condition of no rubbing contact is to be maintained.

Figure 9 shows the effect of face deformation (tilt) on the pressure gradient. The

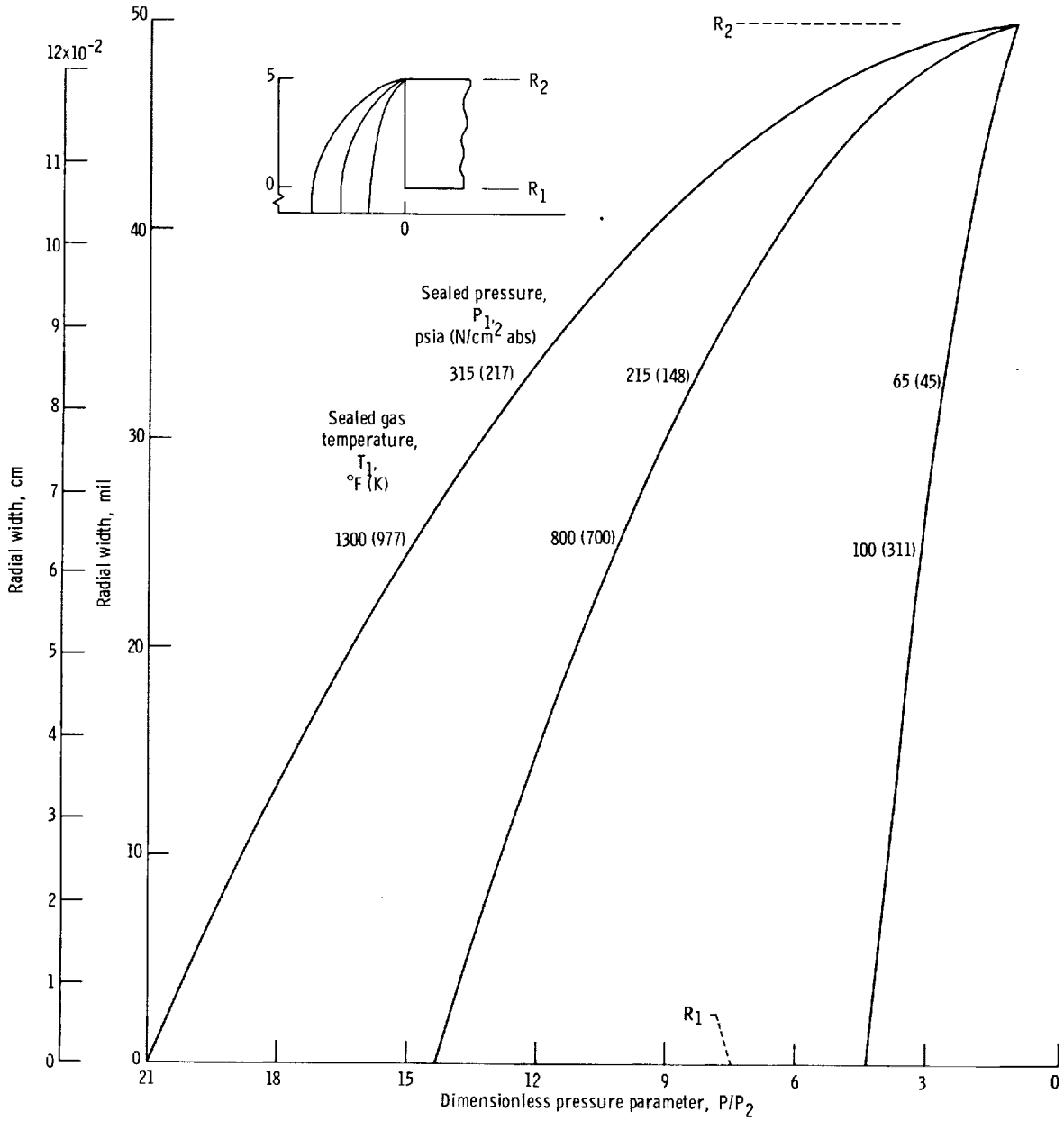

Figure 7. - Gas pressure gradient (profile) within sealing faces. Parallel sealing faces; sump pressure, P_2, 15 psia (10.3 N/cm^2 abs); subsonic flow (Mach number <0.845).

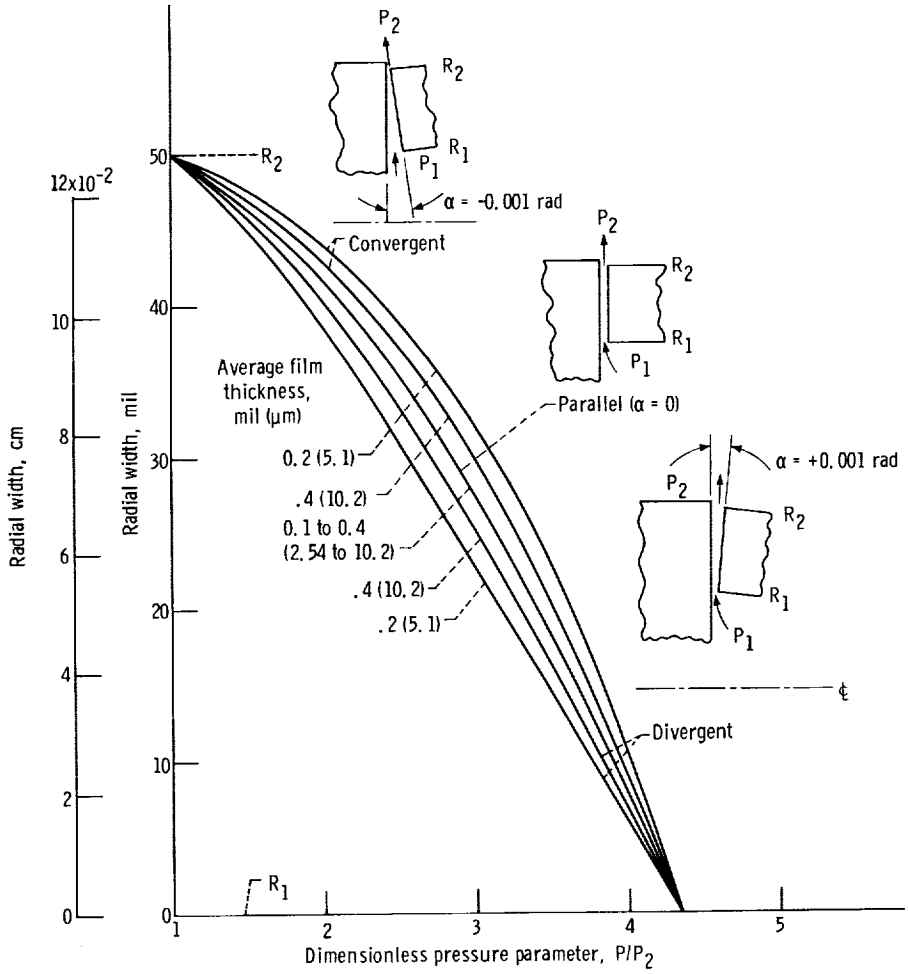

Figure 8. - Pressure ratio as function of average film thickness. Design point 1: sealed pressure, P_1, 65 psia (45 N/cm^2 abs); sealed gas temperature, T_1, 100° F (311 K); sump pressure, P_2, 15 psia (10.3 N/cm^2 abs); radial dam width, 50 mils (0.127 cm).

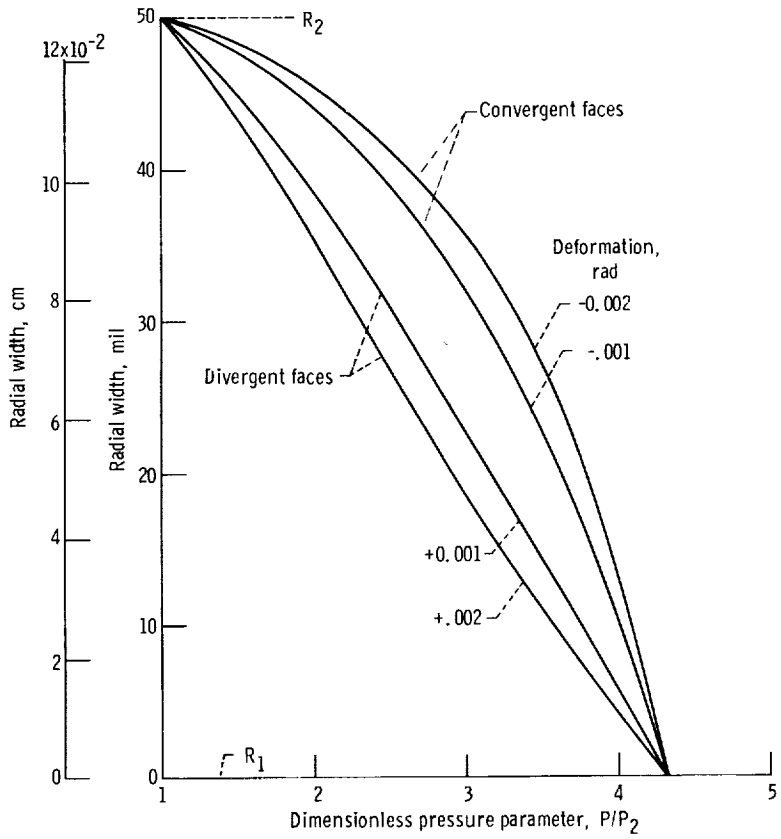

Figure 9. - Effect of face deformation (tilt) on pressure gradient. Design point 1: sealed pressure, P_1, 65 psia (45 N/cm^2 abs); sealed gas temperature, T_1, 100° F (311 K); sump pressure, P_2, 15 psia (10.3 N/cm^2 abs); radial dam width, 50 mils (0.127 cm); average film thickness, 0.2 mil (5.1 μm).

deformations shown, ±0.001 and ±0.002 radian, can readily occur because of thermal gradients. For example, the 0.002-radian deformation amounts to 0.1-mil (0.000254-cm) film thickness change across the 50-mil (0.127-cm) radial dam width. For the convergent film case, an increase in the angle of convergence (increase deformation or tilt) results in a greater area (larger opening force) under the pressure gradient curve. For the case shown (fig. 9), the sealing dam with -0.002-radian deformation has more film stiffness than the dam with the -0.001-radian deformation. For the divergent case, the decrease in opening force (area under curve) is greater for the +0.002-radian deformation as compared to the +0.001-radian deformation. Thus, increasing the convergent deformation increases the positive film stiffness, while increasing the divergent deformation increases the negative film stiffness inherent to divergent faces.

Figure 10 shows the pressure profiles along the sealing dam radial width found using the quasi-one-dimensional computer program for parallel surfaces only. For film

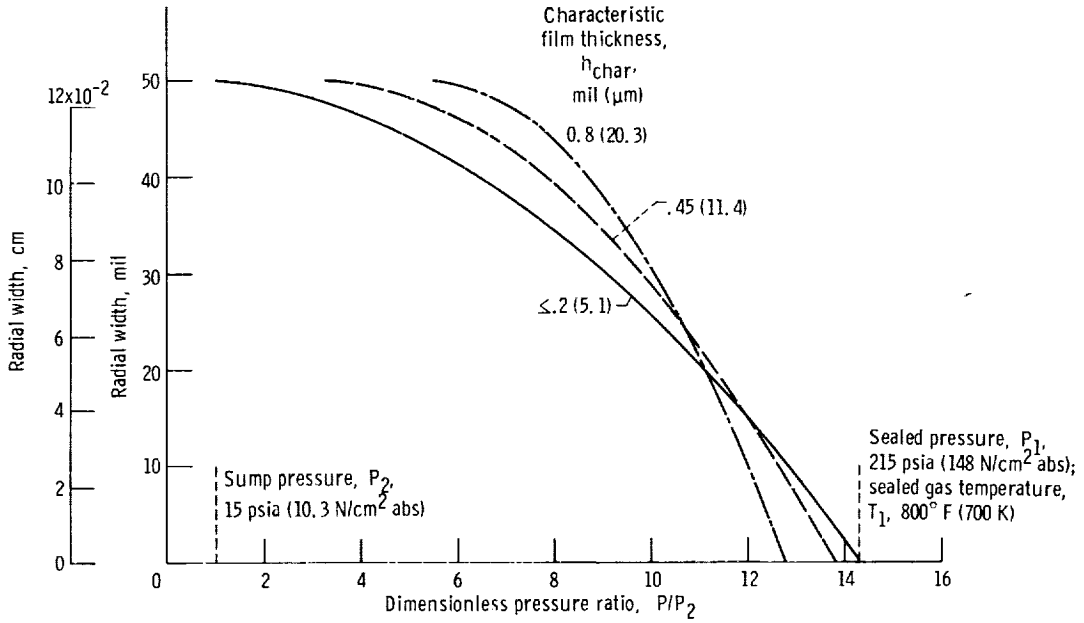

Figure 10. - Pressure ratio variation across sealing dam radial width for several parallel film thicknesses representing subsonic and choked flow conditions. Design point 2.

thickness equal to or less than 0.2 mil (0.00051 cm), the profile does not depend on film thickness. The flow is subsonic, as is found from the isothermal viscous flow analysis in reference 7 and shown in figure 7. When the flow is choked and the mean film thickness increases, the entrance pressure loss becomes significant. The entrance velocity is negligible in subsonic viscous flow; however, under choked conditions, the entrance velocity is no longer negligible. This results in an entrance pressure loss. Also under choked flow conditions, the exit pressure is larger than the sump pressure and increases with film thickness. The pressure expands in an oscillatory manner to the sump pressure in the outer cavity. (This does not significantly affect the radial force balance.)

Sealing Dam Opening Force

The area under the pressure gradient curves (figs. 7 to 10) represents a force which tends to open the seal. This opening force is found by an integration of the pressure distribution across the sealing dam radial width. The marked effect of sealing face deformation can be more directly shown (as compared to figs. 8 and 9) by plotting the opening force as a function of mean film thickness (fig. 11). For illustration, the opening force is plotted for five angular face deformations ($\alpha = 0$, $\alpha = \pm 0.001$, and $\alpha \pm 0.002$

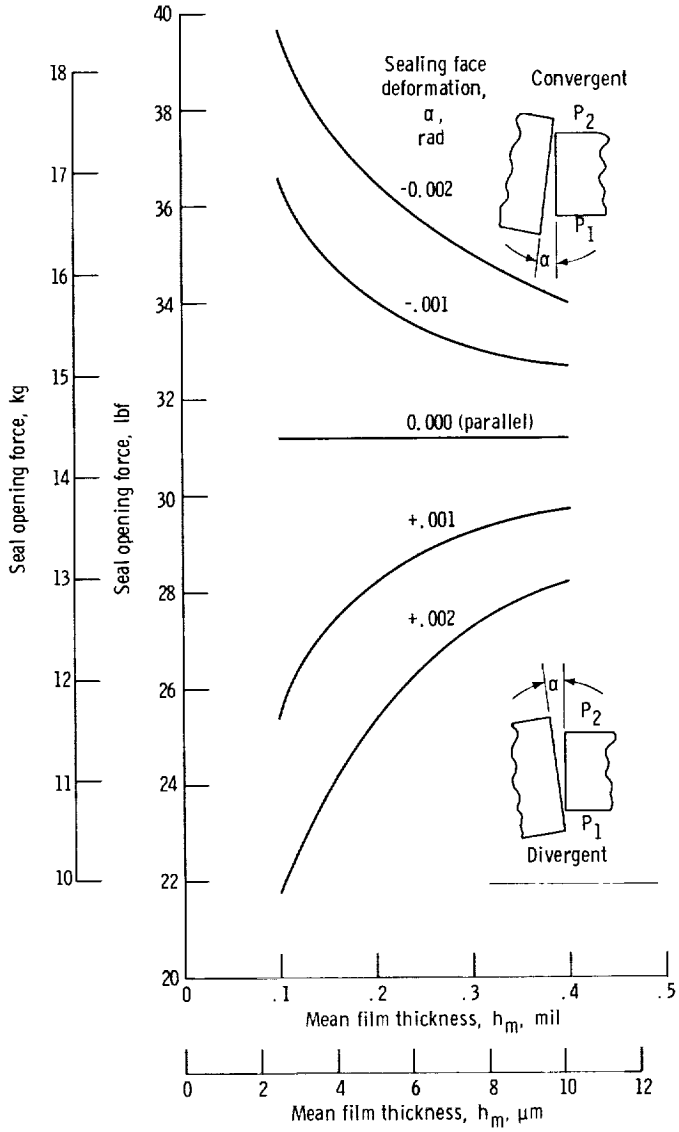

Figure 11. - Effect of sealing face deformation on opening force. Design point 1: sealed pressure, P_1, 65 psia (45 N/cm^2 abs); sealed gas temperature, T_1, 100° F (311 K); sump pressure, P_2, 15 psia (10.3 N/cm^2 abs); radial dam width, 50 mils (0.127 cm).

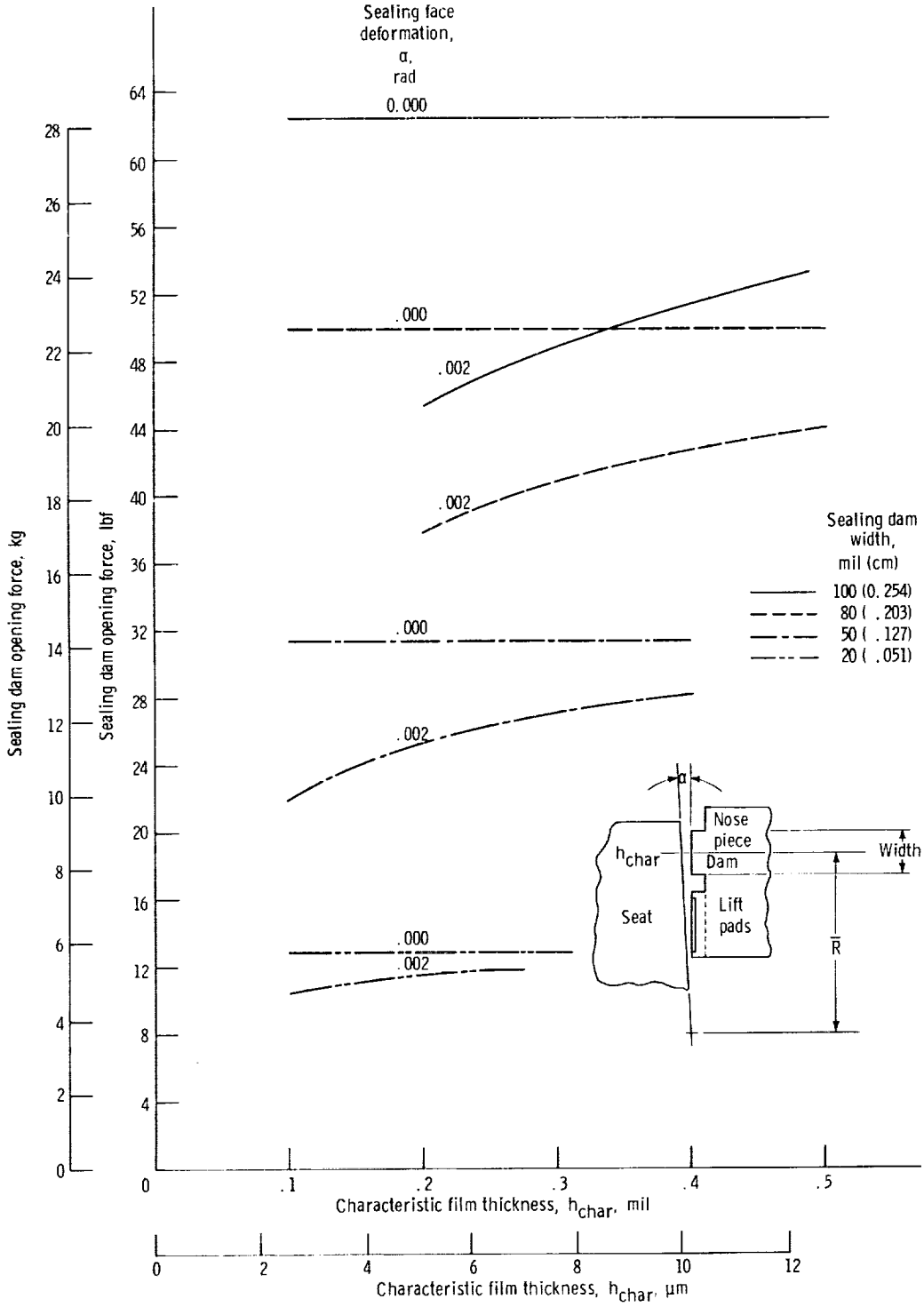

Figure 12. - Effect of seal face radial width (dam) on opening force for parallel film and 2-milliradian tilt. Design point 1: sealed pressure, P_1, 65 psia (45 N/cm^2 abs); sump pressure, P_2, 15 psia (10.3 N/cm^2 abs); sealed gas temperature, T_1, 800° F (700 K).

rad), and for the design point of 65 psia (45 N/cm^2 abs) and 100° R (311 K). As shown in figure 11 the effect of angular deformation is more pronounced as the film thickness decreases; the larger deformation (0.002 rad) has a greater effect on opening force than the smaller deformation of 0.001 radian. As stated previously, for parallel faces the opening force is independent of film thickness; for a convergent film the force increases as the film thickness decreases (positive film stiffness); and for a divergent film the opening force decreases as the film thickness decreases.

The change in seal opening force due to a divergent deformation is of particular interest because the divergent deformation is a natural tendency (due to thermal gradient) in a gas turbine engine (ref. 9). Any decrease in seal opening force due to a divergent deformation must be compensated by the lift pads; the magnitude of opening force changes, therefore, helps to determine the lift pad requirements. Of interest is the effect of seal dam width on seal opening force. This effect is shown in figure 12 in which the opening force is plotted as a function of average film thickness for a divergent deformation of +0.002 radian. Four dam widths (see table III) typical of conventional

TABLE III. - TYPICAL FACE SEAL DAM WIDTHS

Dam width		Opening force change	
mils	cm	lbf	kg
100	0.254	6.3	2.87
80	.203	5.1	2.32
50	.127	3.0	1.36
20	.051	<1.0	<.45

face seals were chosen for comparative purposes. As shown in figure 12, the smallest dam width, 20 mils (0.051 cm), has the smallest opening force change when the film thickness changes. For example, if the film thickness changes from 0.4 mil (0.00102 cm) to 0.2 mil (0.00051 cm), force changes occur as shown in table III. The smaller dam widths are clearly desirable because smaller force changes are produced under dynamic conditions when the film thickness is changing. Thus, the size of the self-acting lift pads can be minimized (the smaller the radial width of the lift pads, the less sensitive the seal is to face deformation effects). However, a comprise must be made on the sealing dam radial width. There is a structural limitation on the width especially for high pressure differentials. Also the mass leakage flow rate is inversely proportional to the sealing dam radial width. Hence, a wide sealing dam is preferred from the leakage standpoint.

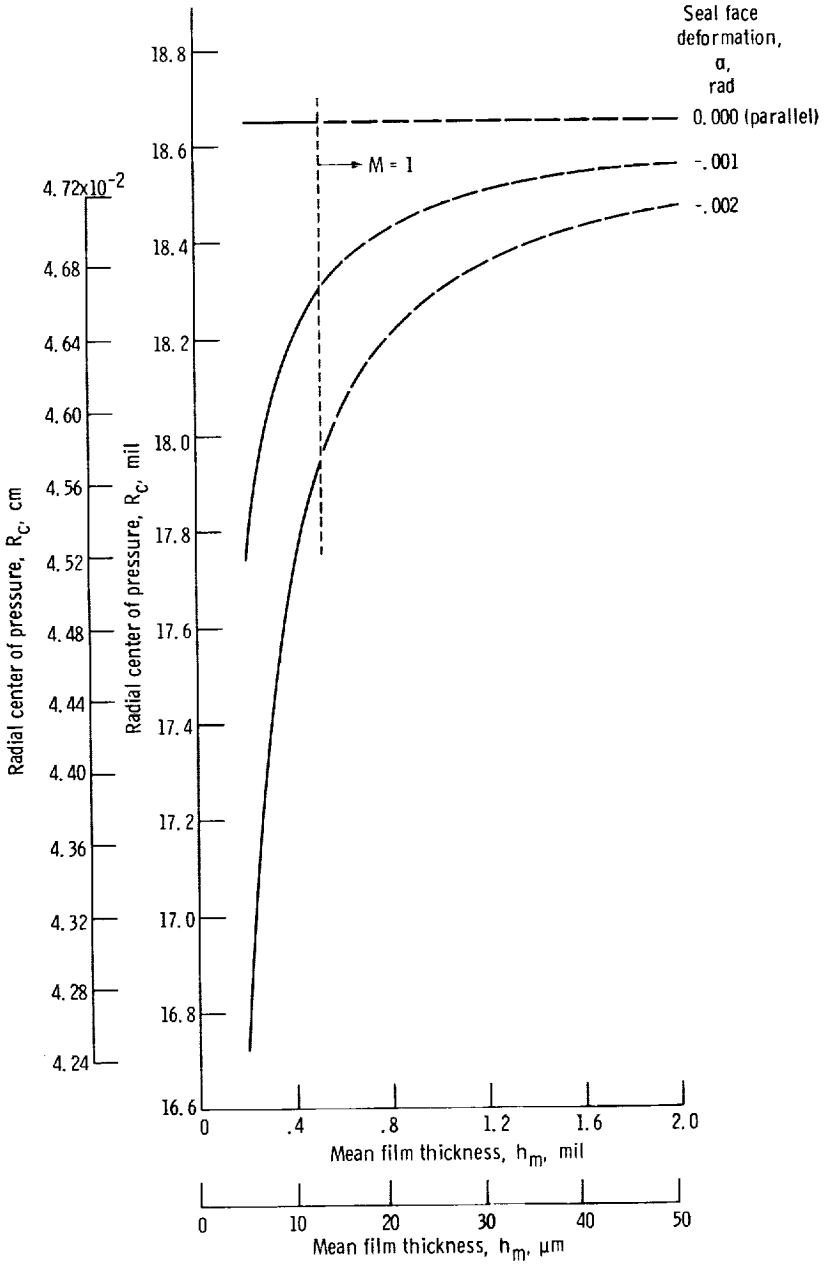

Figure 13. - Center of pressure variation with film thickness and face deformation. Design point 1: sealed pressure, P_1, 65 psia (45 N/cm^2 abs); sealed gas temperature, T_1, 100° F (311 K); sump pressure, P_2, 15 psia (10.3 N/cm^2 abs).

Center of Pressure

The center of pressure is important in determining the net twisting moment acting on the seal nosepiece. The center of pressure in the radial direction is plotted as a function of film thickness in figure 13. Both parallel faces and deformed diverging faces are shown for design point 1. The converging face case would be the mirror image about the parallel case line. There is a severe rate of change in the center of pressure for film thicknesses less than 0.5 mil (0.00127 cm); and, as expected from the pressure profile (fig. 7), the center of pressure is a strong function of the face deformation. At film thicknesses greater than 0.5 mil (0.00127 cm), the flow is choked and the analysis of reference 7 is no longer valid because momentum change effects are neglected. (The quasi-one-dimensional flow analysis is valid for parallel surfaces only.) For film thicknesses greater than 0.5 mil (0.00127 cm), the center-of-pressure values are shown as fictitious quantities computed from reference 7 in order to illustrate qualitative behavior. Both the 1- and 2-milliradian tilt cases show the proper asymptotic behavior to the parallel case at large film thicknesses. This figure illustrates another reason for minimizing the face deformation.

Figure 14 illustrates the radial center-of-pressure variation for design point 1 using the quasi-one-dimensional flow computer program. At low values of film thickness) subsonic flow), the center of pressure is the same as the value obtained from the isothermal viscous flow analysis (18.65 mils, 47.37 cm), which is valid for Mach numbers less than $1/\sqrt{\gamma}$. For film thickness larger than the critical choking film thickness, the center of pressure increases at a lesser rate and eventually, at larger film thicknesses than shown, would be asymtotic to a dimensionless value of 0.500.

Gross Seal Characteristics

Since the sealing dam has been analyzed and the self-acting-geometry load against film thickness characteristics were found in the companion paper, reference 6, the gas film seal operating characteristics, including film stiffness, can be found for the three design points. The self-acting-geometry load capacity against film thickness characteristics are shown in figures 15 and 16.

The seal is balanced by equating the closing force with the opening force. The closing force is comprised of the spring force and a hydrostatic closing force. A spring force of 6.6 pounds force (3.0 kg) was chosen to be the minimum force required to balance the nosepiece inertia force at startup. The hydrostatic closing force is found by trial and error. The outer diameter of the hydrostatic force area (known as the balance diameter and shown in fig. 2) is chosen such that the seal leakage is tolerable and the

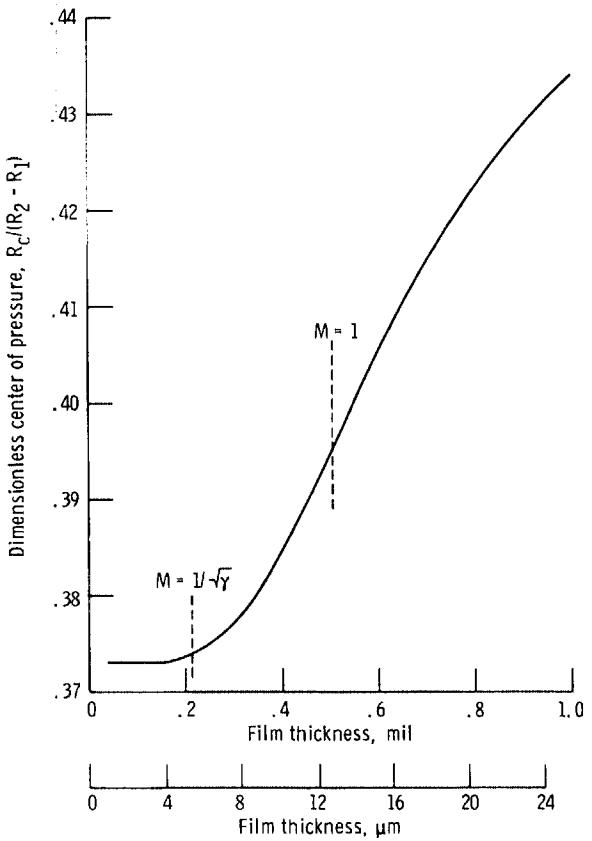

Figure 14. - Center of pressure variation as a function of parallel film thickness representing subsonic and choked flow conditions. Design point 1: sealed pressure, P_1, 65 psia (45 N/cm^2 abs); sealed gas temperature, T_1, 100° F (311 K); sump pressure, P_2, 15 psia (10.3 N/cm^2 abs).

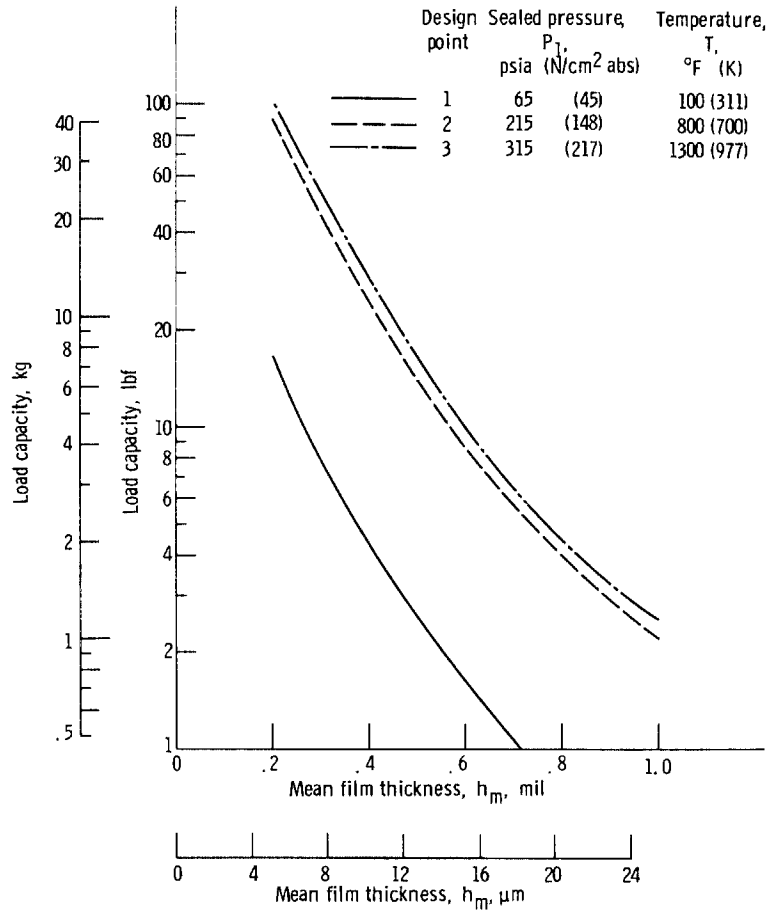

Figure 15. - Load capacity of shrouded self-acting lift pads as function of film thickness. Number of pads, 20; recess-length-to-land-length ratio, 1.4. (Data from ref. 6.)

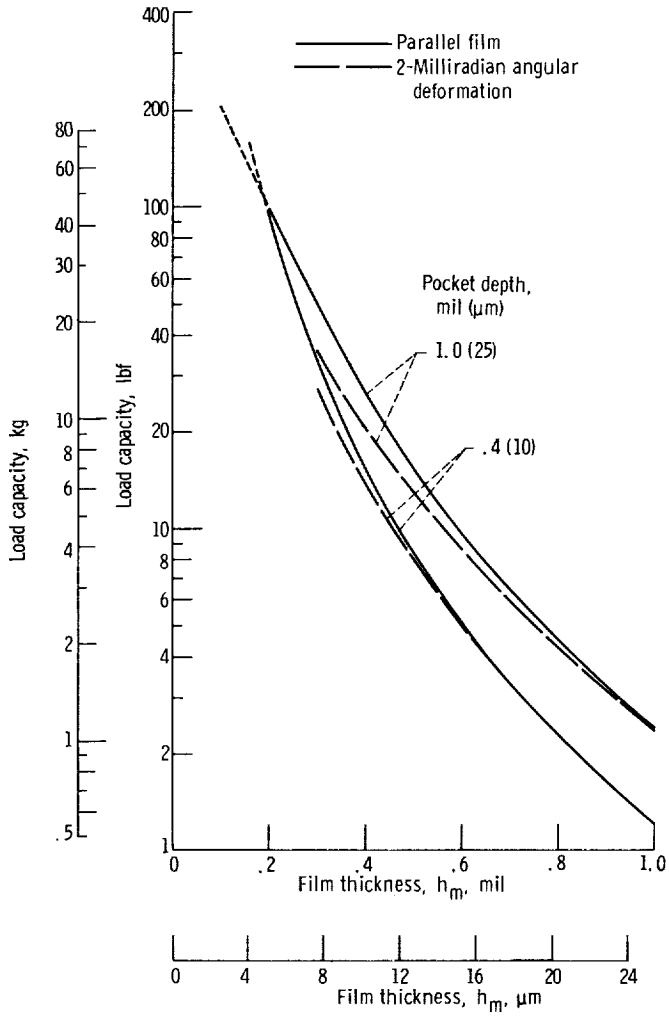

Figure 16. - Load capacity of self-acting geometry as function of angular deformation. Sealed pressure, P_1, 315 psia (217 N/cm^2 abs); sealed gas temperature, T_1, 1300° F (977 K); sliding velocity, 400 feet per second (122 m/sec); number of pads, 20; recess-length-to-land-length ratio, 1.4; recess depths, 1.0 and 0.4 mil (25 and 10 μm). (Data from ref. 6.)

seal withstands anticipated face deformations.

A 50-mil (0.127-cm) radial dam width was chosen because this dam width appeared to satisfy the design compromises. The results for parallel surfaces are summarized in table IV. A leakage of 25 SCFM (1.18×10^{-3} SCMS) or less can be expected for all three design points. This is about an order of magnitude less than that achieved by conventional labyrinth seal practice.

TABLE IV. - SUMMARY OF GROSS SHAFT FACE SEAL (WITH SELF-ACTING LIFT AUGMENTATION) CHARACTERISTICS DETERMINED FROM A FORCE BALANCE (PARALLEL FILM)

Design point	Closing force, lbf (kg)		Total force, lbf (kg)	Opening force, lbf (kg)		Operating gap, mils (μm)	Leakage flow rate, SCFM (SCMS)
	Hydrostatic	Spring		Sealing dam	Pad		
1	36.1 (16.4)	6.6 (3.0)	42.7 (19.4)	31.3 (14.2)	11.4 (5.18)	0.25 (6.30)	0.83 (3.92×10^{-4})
2	144.4 (65.6)	6.6 (3.0)	151 (68.7)	141.8 (64.5)	9.2 (4.19)	0.59 (14.9)	17.5 (8.26×10^{-4})
3	216.7 (98.5)	6.6 (3.0)	223.3 (101.5)	214.8 (97.6)	8.5 (3.87)	0.63 (15.9)	25 (1.18×10^{-3})

SUMMARY OF RESULTS

A design analysis was made of seal leakage flow rate and radial pressure distribution in a shaft face seal with self-acting lift pads using the best available mathematical models. The seal had a 6.5-inch (16.5-cm) nominal diameter dam. Three design conditions typical of sump seals in advanced aircraft gas turbines were considered. These design conditions exceed the limits of conventional rubbing-contact face seal operation; an alternate conventional face seal - labyrinth seal system approach would yield too high a leakage flow rate and/or a more complex seal system. The investigation included studying the effects of sealing face radial width and the effect of sealing face angular deformation. The following pertinent results were obtained:

1. The shaft face seal with self-acting lift pads force balance indicates that this nonrubbing-contact face seal design is technically feasible and that leakage flow rates an order of magnitude less than that obtained in conventional labyrinth seal practice are possible.

2. Slight face angular deformation (i.e., ±0.001 rad) has a significant effect on the

pressure gradient within the sealing faces; thus, the seal opening force and radial center of pressure are markedly affected.

3. A narrow radial sealing face width (dam) is preferred because the narrow face has less effect on the opening force when the commonly occurring diverging radial face deformation occurs. However, both for structural and mass leakage path reasons, a large radial dam width is desirable. Hence, the sealing dam width must be compromised. The leakage of the selected 50-mil (0.127-cm) radial dam width is within the design goal of 25 SCFM (1.18×10^{-3} SCMS) or less for all three design points.

4. For the design configurations and operating conditions studied, the flow at the exit of the sealing dam was choked. This was due to the minimum operating gap necessary for satisfactory seal operation. The leakage flow was even choked for the first design point where the pressure ratio across the seal was only 4 to 1.

Lewis Research Center,
National Aeronautics and Space Administration,
Cleveland, Ohio, July 23, 1970,
126-15.

APPENDIX - SYMBOLS

B	constant, $h_m - \left[\alpha(R_2 - R_1)/2\right]$
F	sealing dam force, lbf; kg
$\overline{f}$	mean friction factor
h	film thickness, mil; cm
h_{char}	characteristic film thickness, $(h_1^2 h_2^2/h_m)^{1/3}$, mil; cm
L	sealing dam circumferential length, mil; cm
M	Mach number
P	pressure, psi; N/m^2
P_o	outboard vent pressure
P_1	sealed pressure
P_2	sump pressure
P_3	hot turbine gas pressure
P_1'	static pressure at sealing dam entrance
P_2'	static pressure at sealing dam exit
Q	net leakage (volume) flow rate, SCFM; SCMS
$\mathcal{R}$	gas constant, universal gas constant/molecular weight, ft-lbf/(lbm)(^oR); J/(kg)(K)
R	radius, mil; cm
ΔR	sealing dam radial width, $R_2 - R_1$, mil; cm
R_c	center of pressure in radial or x-direction, mil; cm (referenced from inner diameter)
Re	Reynolds number
r	radial direction coordinate
T	temperature, ^oF; K
V	mean relative surface speeds of seal dam surfaces, ft/sec; m/sec
x	coordinate in pressure gradient direction (radial direction)
y	coordinate across film thickness
z	shear flow coordinate in Cartesian system
α	relative inclination angle of sealing dam surfaces, rad
γ	specific-heat ratio, C_p/C_v
μ	absolute or dynamic viscosity, lbf-sec/ft^2; N-sec/m^2
ρ	density, (lbf)(sec^2)/ft^4; kg/m^3

Subscripts:

m	mean
1	inner cavity
2	outer cavity

REFERENCES

1. Parks, A. J.; McKibben, R. H.; Ng, C. C. W.; and Slayton, R. M.: Development of Mainshaft Seals for Advanced Air Breathing Propulsion Systems. Rep. PWA-3161, Pratt & Whitney Aircraft (NASA CR-72338), Aug. 14, 1967.

2. Shevchenko, Richard P.: Shaft, Bearing and Seal Systems For a Small Engine. Paper 670064, SAE, Jan. 1967.

3. McKibben, A. H.; and Parks, A. J.: Aircraft Gas Turbine Mainshaft Face Seals - Problems and Promises. Paper FICFS-28, ASLE, May 1969.

4. Hawkins, R. M.; McKibbin, A. H.; and Ng, C. C. W.: Development of Compressor Seals, Stator Interstage Seals, and Stator Pivot Seals in Advanced Air Breathing Propulsion Systems. Rep. PWA-3147, Pratt & Whitney Aircraft (NASA CR-95946), July 20, 1967.

5. Hawkins, R. M.: Development of Compressor End Seals, Stator Interstage Seals, and Stator Pivot Seals in Advanced Air Breathing Propulsion Systems. Rep. PWA-2875, Pratt & Whitney Aircraft (NASA CR-83786), July 20, 1966.

6. Zuk, John; Ludwig, Lawrence P.; and Johnson, Robert L.: Design Study of Shaft Face Seal With Self-Acting Lift Augmentation. I - Self-Acting Pad Geometry. NASA TN D-5744, 1970.

7. Zuk, John; and Smith, Patricia J.: Computer Program for Viscous, Isothermal Compressible Flow Across a Sealing Dam With Small Tilt Angle. NASA TN D-5373, 1969.

8. Zuk, John; and Ludwig, Lawrence P.: Investigation of Isothermal, Compressible Flow Across a Rotating Sealing Dam. I - Analysis. NASA TN D-5344, 1969.

9. Johnson, Robert L.; and Ludwig, Lawrence P.: Shaft Face Seal With Self-Acting Lift Augmentation For Advanced Gas Turbine Engines. NASA TN D-5170, 1969.

NASA-Langley, 1970 — 15 E-5796